

# MM-Interleaved: Interleaved Image-Text Generative Modeling via Multi-modal Feature Synchronizer

Changyao Tian<sup>2,1,\*†</sup>, Xizhou Zhu<sup>3,4,1\*</sup>, Yuwen Xiong<sup>5,1\*</sup>, Weiyun Wang<sup>6,1†</sup>, Zhe Chen<sup>7,1†</sup>, Wenhai Wang<sup>2,1</sup>, Yuntao Chen<sup>8</sup>, Lewei Lu<sup>4</sup>, Tong Lu<sup>7</sup>, Jie Zhou<sup>3</sup>, Hongsheng Li<sup>2</sup>, Yu Qiao<sup>1</sup>, Jifeng Dai<sup>3,1</sup>✉  
<sup>1</sup>OpenGVLab, Shanghai AI Laboratory <sup>2</sup>MMLab, The Chinese University of Hong Kong  
<sup>3</sup>Tsinghua University <sup>4</sup>SenseTime Research <sup>5</sup>University of Toronto <sup>6</sup>Fudan University  
<sup>7</sup>Nanjing University <sup>8</sup>CAIR, HKISI, CAS

<https://github.com/OpenGVLab/MM-Interleaved>

## Abstract

Developing generative models for interleaved image-text data has both research and practical value. It requires models to understand the interleaved sequences and subsequently generate images and text. However, existing attempts are limited by the issue that the fixed number of visual tokens cannot efficiently capture image details, which is particularly problematic in the multi-image scenarios. To address this, this paper presents MM-Interleaved, an end-to-end generative model for interleaved image-text data. It introduces a multi-scale and multi-image feature synchronizer module, allowing direct access to fine-grained image features in the previous context during the generation process. MM-Interleaved is end-to-end pre-trained on both paired and interleaved image-text corpora. It is further enhanced through a supervised fine-tuning phase, wherein the model improves its ability to follow complex multi-modal instructions. Experiments demonstrate the versatility of MM-Interleaved in recognizing visual details following multi-modal instructions and generating consistent images following both textual and visual conditions. Code and models are available at <https://github.com/OpenGVLab/MM-Interleaved>.

## 1. Introduction

Interleaved image-text data, where the text and images are related in content and intertwined in layout, is very common on the internet. As an extension of image-text pairs widely used in previous multi-modal models [21, 22, 37, 70, 82],

\* Equal contribution.

† This work is done when Changyao Tian, Weiyun Wang, and Zhe Chen are interns at Shanghai AI Laboratory.

✉ Corresponding author (daijifeng@tsinghua.edu.cn).

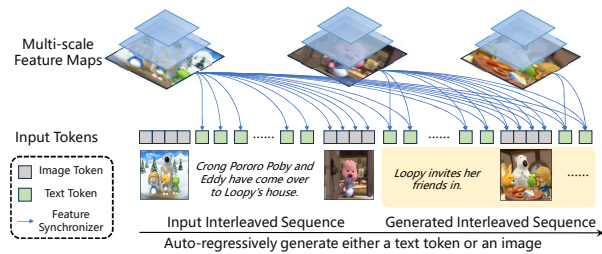


Figure 1. **Illustration of multi-modal feature synchronizer.** In the auto-regressive generation of interleaved image-text sequences, besides interacting with low-resolution image tokens with self-attention, tokens in MM-Interleaved could also use the multi-modal feature synchronizer to cross-attend multi-scale high-resolution image features. The multi-modal feature synchronizer ensures the cross attention will have exactly the same causal relation between image and text tokens.

the interleaved format not only covers a broader range of data but also presents more complex information structures. Developing multi-modal models that can simultaneously understand and generate such interleaved image-text data has significant research value and practical application potential. It broadens the application scope of previous multi-modal models [83] and enables more unified processing of multi-modal data, bringing previously isolated research fields such as text-to-image generation [71, 74] and visual question-answering [48, 53] together.

With recent progress in multi-modal modeling with Large Language Models (LLMs) [7, 64], exploring how LLMs can be leveraged for interleaved image-text modeling has become increasingly attractive. A core challenge of interleaved multi-modal LLMs is how to effectively handle multiple images within the limited context length of LLMs. In most multi-modal LLMs, images are encoded as visual tokens from an image tokenizer (also known as image encoder) and fed into LLMs together with text tokens [18, 40, 43, 83]. To reduce computational demands

and the required context length of LLMs, Perceiver Resamplers [3] are commonly used to map each image from up to 1024 tokens to a fixed number of visual tokens (*e.g.*, 32 or 64 tokens) as in Fig. 2. Due to the relatively small token number, critical image details may be overlooked, especially in tasks requiring fine-grained observation. Increasing the number of visual tokens [55, 99] can address this issue to some extent. While the context length of LLMs is typically limited, allocating a large number (*e.g.*, 2890 in [84]) of visual tokens per image would pose a significant limitation in multi-image scenarios.

We note that the main problem is that the Perceiver Resampler only takes image features as input and is context-insensitive. It compresses each input image to a fixed number of tokens, which makes it harder or even impossible to preserve all information required and fulfill all needs for subsequent generation. In contrast, allowing intermediate layers in decoder networks to dynamically extract a small amount of relevant information from the images can compensate for this information loss. Such a dynamic extraction mechanism should also efficiently handle scenarios requiring multiple images and high-resolution feature maps.

Motivated by this, we designed a fine-grained multi-modal feature synchronizer based on the deformable sparse attention [110]. As shown in Fig. 1, it enables the multi-modal LLMs to observe multi-scale high-resolution image features from multiple images efficiently. This mechanism facilitates the extraction of fine-grained image details with only a small number of input visual tokens, which is particularly applicable to interleaved image-text scenarios with multiple images.

Based on this module, we propose MM-Interleaved, a novel end-to-end generation model for processing interleaved image-text data, as shown in Fig. 3. Images and text are first mapped into tokens through their respective tokenizers (*i.e.*, image encoder and word embedding) and then fed to the LLM, arranged in their original order. A special token  $\langle \text{B}\circ\text{I} \rangle$  is introduced to represent “Begin of Image”. When the LLM processes image and text sequences, each token in the intermediate layers directly observes multi-image and multi-scale feature maps from the previous context through the proposed feature synchronizer module. After being processed by the LLM, the features of the text tokens predict the next text word. When the  $\langle \text{B}\circ\text{I} \rangle$  token is predicted, an image decoder based on diffusion models is used to predict the next image. All previous LLM output features are passed into the image decoder to generate images. Each pixel in the intermediate layers of the decoder can also extract details of the previous image through the proposed synchronizer module.

Our models are pre-trained on a mixture of image-text pairs and interleaved image-text sequences. We do not use any in-house data. Similar to previous multi-modal LLMs, supervised fine-tuning can further enhance our model ca-

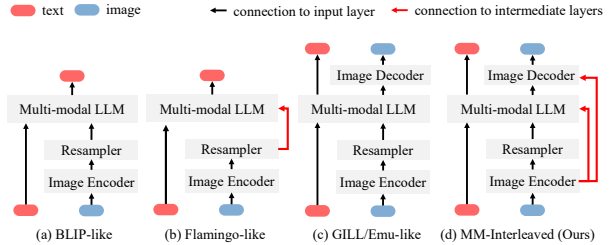


Figure 2. **Comparison of different types of image-text generative modeling.** (a) and (b) can only generate text. (c) and (d) can generate both images and text. All types except (d) are limited by the fixed number of visual tokens extracted by context-insensitive Resampler, which can not efficiently capture image details and is problematic in multi-image scenarios.

pabilities. Thanks to end-to-end generative modeling, fine-tuning can be applied to both text and image generation. Our model is fine-tuned on several tasks, including visual question-answering, image caption, referring expression grounding, text-to-image generation, segmentation-to-image translation, and visual storytelling. Compared with previous image-to-text and text-to-image methods, our model achieves competitive results and shows higher token efficiency. Compared with joint image and text generation models, we set the new SotA results for a wide range of tasks. Overall, MM-Interleaved can handle interleaved image-text inputs and recognize fine-grained details across multiple images to produce accurate textual descriptions and visually consistent images, demonstrating the potential of high-performance multi-modal models that can understand and generate interleaved image-text content.

## 2. Related Work

**Modeling of Paired Image-Text Data** plays an important role in the progress of multi-modal research in recent years. [24, 37, 76] has released a series of public large-scale image-text pairs datasets. Based on these data, models trained by image-text contrastive learning [39, 50, 70, 82] have been proven able to recognize and understand open-world semantics. Subsequent work [46, 93, 97, 111] further incorporates the text generation tasks such as image captioning. Some other works [71, 74] were proposed to generate images based on text prompts. The latest progress of LLMs [64, 65] has created a new era, leading to the emergence of many LLM-based multi-modal models trained using image-text pairs [48, 53, 90, 91]. For example, [53] connect pre-trained LLMs and vision foundation models with linear projections to build powerful multi-modal text-generation models.

**Modeling of Interleaved Image-Text Data** has received increasing attention recently. [3, 33] were the first to focus on understanding such data relying on non-public datasets. To promote the development of this field, [45, 109] re-

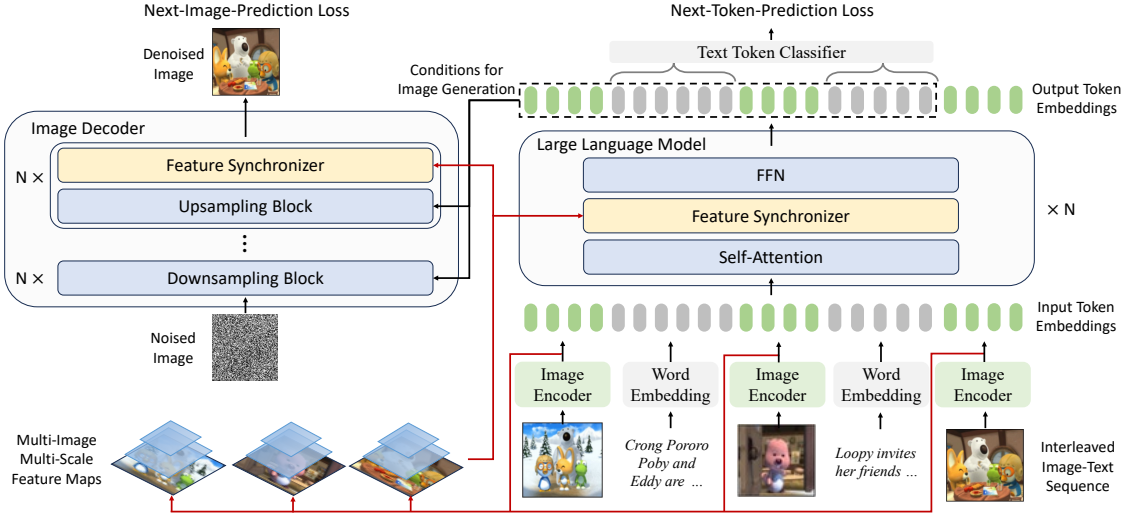


Figure 3. **Architecture of the proposed MM-Interleaved Model.** The red lines represent how the multi-scale image features are generated and utilized. MM-Interleaved incorporates image encoder to both extract high-resolution multi-scale image features and map each image into a fixed number of low-resolution visual tokens. These visual tokens are fed into the multi-modal LLM along with text tokens. LLM uses the feature synchronization module to extract high resolution image details, and auto-regressively generates text tokens. After that, a DM-based image decoder generates next image conditioned on the previous context features from LLM as well as the multi-scale image features from the feature synchronization module.

lease public and large-scale interleaved image-text datasets. More works [101, 103] have begun to focus on understanding the interleaved data. Nevertheless, their generative capabilities remain limited to text. [18, 43, 83, 99] have initially attempted to generate images and text in the interleaved context concurrently. [43, 83] involve a two-stage generation process, where text and image are only generated in the first and second stages, respectively. [99] uses VQ-VAE [86] to convert images into discrete tokens, facilitating token-level auto-regressive modeling as traditional language modeling. However, it primarily focuses on image generation capabilities and exhibits notable weaknesses in image understanding. DreamLLM [18], a concurrent work to ours, also focuses on single-stage end-to-end modeling using raw image pixels as input. Despite these efforts, they only feed image information at the input of LLMs, which are limited by the problem that fixed number of visual tokens cannot efficiently describe image details.

**Integrating Image Details into LLMs** is important for multi-modal LLMs. Most works use Perceiver Resamplers [3, 48, 107] to extract image information via cross-attention, mapping each image into a fixed number of visual tokens. For example, [3] equips Resamplers in the intermediate layers of LLMs, injecting extracted image features into LLMs through gated residual connections. [48, 107] introduces Resamplers at the bottom of LLM to insert the extracted visual tokens into the input text sequences. While these methods achieve good performance, image details may be overlooked due to the small number (e.g., 32 or 64) of visual tokens. To preserve more image details,

[6, 10, 53, 55] increase the number of input visual tokens per image to hundreds. [84] further increases this number to 2,890. Although it mitigates information loss, the computational and memory demands of LLMs are significantly increased. Increasing the number of visual tokens per image is particularly problematic in multi-image scenarios, where multiple images naturally require more visual tokens, making it hard to use for interleaved image-text data.

## 3. Method

### 3.1. Task Formulation

To build an end-to-end generative model for interleaved image-text data. We first consider an interleaved image-text sequence  $X = \{x_1, x_2, x_3, \dots\}$ , where each element  $x_n$  is either a text token (denoted as  $x_n^L$ ) or a whole image (denoted as  $x_n^V$ ). Text and images are arranged in the order in which they appear in the original content. In multi-modal LLMs, a common practice is first extracting embedding for each text token and each image before being fed into LLMs, i.e.,  $e_n^L = \mathcal{E}_L(x_n^L)$  and  $e_n^V = \mathcal{E}_V(x_n^V)$ , where  $\mathcal{E}_L$  denotes word embedding following standard practices in NLP.  $\mathcal{E}_V$  is typically an image encoder (e.g., ViTs [19]) followed by a Perceiver Resampler [3] to map each image to a fixed number of tokens. Then, the generative modeling is trained to maximize the log-likelihood of the multi-modal sequence,

given by:

$$\begin{aligned}
\log p(X) &= \sum_n \log p(x_n | x_1, x_2, \dots, x_{n-1}) \\
&= \sum_n \log p(x_n | e_1, e_2, \dots, e_{n-1}) \\
&= \sum_{n \in \mathcal{I}_L} \log p(x_n^L | e_{<n}) + \sum_{n \in \mathcal{I}_V} \log p(x_n^V | e_{<n}),
\end{aligned} \tag{1}$$

where  $\mathcal{I}_L$  and  $\mathcal{I}_V$  represent the index sets for text tokens and images within the sequence, respectively.  $<n$  in the subscript represents the abbreviation of  $\{1, 2, \dots, n-1\}$ . The following paragraphs provide explanations of Eq. (1).

**Text Generation with Multi-modal Condition.** The log-likelihood  $\log p(x_n^L | e_{<n})$  is similar to traditional causal language modeling, except that the condition also includes previous images. Recent works [48, 53, 90, 91] have demonstrated the effectiveness of using LLMs for processing additional visual inputs. They apply a linear classifier on top of the LLMs. The loss function for text generation is

$$L_{\text{NTP}}(x_n^L | e_{<n}) = -\bar{x}_n^L \cdot \log \text{softmax}(W \cdot \mathcal{D}_{\text{LM}}(e_{<n})), \tag{2}$$

where  $W$  is the linear classification weight,  $\mathcal{D}_{\text{LM}}$  denotes the LLM network (e.g., LLaMA [85]),  $\bar{x}_n^L$  is the one-hot vector indicating the ground-truth text token.

**Image Generation with Multi-modal Condition.** Maximizing the log-likelihood  $\log p(x_n^V | e_{<n})$  aligns with the denoising-diffusion process [54], which recently achieves widespread success in image generation. When conditional inputs  $x_{<n}$  are all text, this is identical to text-to-image diffusion models, where maximizing the log-likelihood is defered as minimizing the diffusion modeling loss as

$$L_{\text{NIP}}(x_n^V | e_{<n}) = \mathbb{E}_{\epsilon, t} \|\epsilon - \mathcal{D}_{\text{DM}}(x_{n,t}^V, t, \mathcal{D}_{\text{LM}}(e_{<n}))\|^2, \tag{3}$$

where  $\mathcal{D}_{\text{LM}}$  is the language model encoding text inputs,  $\mathcal{D}_{\text{DM}}$  is the diffusion model for image denoising.  $x_{n,t}^V$  is the noisy version of the original image at the denoising step  $t$ , and the denoising network  $\mathcal{D}_{\text{DM}}$  is trained to predict the noise  $\epsilon$ . We found that such modeling is also applicable when conditional input is interleaved image-text data.

Note that our modeling allows for the flexible combination of different language models, image encoders, and image decoders to fully leverage a variety of pre-trained models. It does not need to insert additional special tokens specifically for image generation into LLMs. The whole framework can be optimized end-to-end.

### 3.2. Architecture

Building upon the task formulation in Sec. 3.1, we propose a novel multi-modal architecture for processing interleaved image-text data. It integrates a Visual Foundation Model (VFM), a Large Language Model (LLM), and a Diffusion

Model (DM). This integration aims to excel in both understanding and generation tasks of text and images by leveraging the strengths of each model type. As illustrated in Fig. 3, our architecture comprises three key components:

(1) **VFM-based Image Tokenizer**  $\mathcal{E}_V$  that maps each image  $x^V \in \mathbb{R}^{H \times W \times 3}$  (e.g.,  $H = W = 224$ ) into a fixed number of visual tokens  $e^V \in \mathbb{R}^{N \times C}$  ( $N = 32$  by default).  $C$  is the channel dimension. It consists of a pre-trained vision foundation model (e.g., CLIP-ViT [70]) for feature extraction and a Perceiver Resampler [3] to reduce the number of visual tokens. We also use a ViT-Adapter [12] to extract multi-scale image features  $F^V \in \mathbb{R}^{(\sum_{i=1}^L H_i \times W_i) \times C}$  for fine-grained feature fusion in subsequent networks, where  $L = 4$  and  $H_i = \frac{H}{2^{i+1}}$ ,  $W_i = \frac{W}{2^{i+1}}$  by default.

(2) **LLM-based Multi-modal Model**  $\mathcal{D}_{\text{LM}}$  that extracts context features from the interleaved image-text sequences. A pre-trained LLM (e.g., Vicuna [105]) is utilized. Its input sequence  $E \in \mathbb{R}^{K \times C}$  is a concanation of embeddings  $(e_1, e_2, \dots)$ , where  $e_n$  is either a word embedding  $e_n^L \in \mathbb{R}^{1 \times C}$  or an image embedding  $e_n^V \in \mathbb{R}^{N \times C}$ .  $K$  is the total number of input tokens. We also introduce a fine-grained feature synchronizer module for letting the intermediate layers in  $\mathcal{D}_{\text{LM}}$  directly access and extract multi-scale image features on demand.

(3) **DM-based Image Decoder**  $\mathcal{D}_{\text{DM}}$  that generates the image based on previous image-text sequences. A pre-trained diffusion model (e.g., Stable Diffusion [74]) is utilized. To provide the conditional inputs for  $\mathcal{D}_{\text{DM}}$ , Resampler [3] is employed to map the output features from LLM to a fixed number of conditional tokens. The fine-grained feature synchronizer module is also used here for providing detailed visual conditions, which is very useful for tasks requiring visual alignment (e.g., image translation).

Then we introduce the details of the proposed architecture.

**Multi-image and Multi-scale Feature Synchronizer (MMFS).** The MMFS module is designed to dynamically capture image details from multiple images in an interleaved context. It leverages the Deformable Attention [110] mechanism to achieve efficient and sparse image attention. As is shown in Fig. 4, given a query token that requires detailed image features, the MMFS module only attends to a small set of sampling points around a reference point on the reference images. Let  $f_q \in \mathbb{R}^C$  represent the features of the query token.  $\hat{p}_q \in [0, 1]^2$  denotes the relative image coordinate of its reference point. By default,  $\hat{p}_q = (0.5, 0.5)$  corresponds to the center of the images.  $\{F_m^V\}_{m=1}^M$  are the multi-image multi-scale feature maps, where  $F^V$  is the multi-scale feature extracted by the image tokenizer,  $M$  is the number of reference images. The

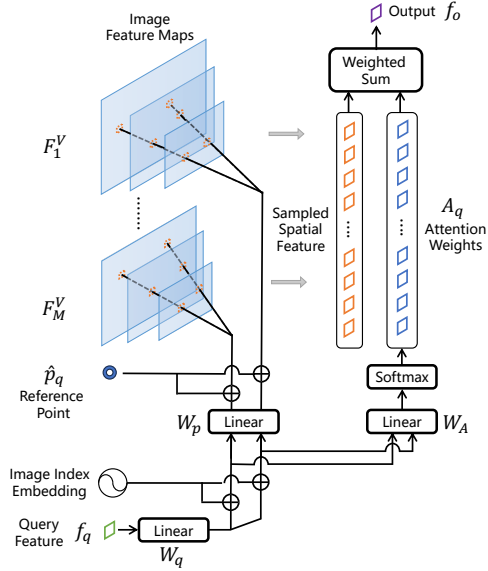


Figure 4. **Architecture of the MMFS module.** The query feature is passed through a linear layer and added to the image index embedding. Two linear layers are used to predict the sampling offsets and unnormalized attention weights of each image respectively. The sampling offsets are added with the query’s reference point to form the corresponding sampling locations, which are shared and rescaled across all feature maps of the same image. The output feature is the weighted sum of the sampled spatial features from these points.

output feature  $f_o \in \mathbb{R}^C$  is given by

$$\begin{aligned}
 q^{(m)} &= W_q \cdot f_q + \text{PosEmbed}(m), \\
 p_q^{(m)} &= W_p \cdot q^{(m)} + \hat{p}_q, \quad A_q^{(m)} = W_A \cdot q^{(m)}, \\
 p_q &= \text{Concat}(p_q^{(1)}, \dots, p_q^{(M)}). \\
 A_q &= \text{softmax}(\text{Concat}(A_q^{(1)}, \dots, A_q^{(M)})). \\
 f_o &= \text{DeformAttn}(\{F^V\}_{m=1}^M, A_q, p_q),
 \end{aligned} \tag{4}$$

where  $\text{PosEmbed} \in \mathbb{R}^{\bar{M} \times C}$  is a learnable positional embedding,  $m$  indexes from the maximum of  $\bar{M}$  reference images.  $W_q, W_p, W_A$  are learnable linear projection weights. The coordinate of sampling points  $p_q^{(m)}$  and the corresponding attention weights  $A_q^{(m)}$  are first calculated for each image separately. Then, the attention weights are normalized among different images via the softmax function. The DeformAttn operator extracts feature at coordinates  $p_q \in \mathbb{R}^{M \times L \times K \times 2}$  from the corresponding feature map, and performs a weighted summation according to  $A_q \in \mathbb{R}^{M \times L \times K}$ . Here,  $L$  and  $K$  denote the number of multi-scale feature levels and sampling points per feature map, respectively.

MMFS can be applied to both image and text decoding, avoiding information bottlenecks caused by the widely used Resamplers in multi-modal LLMs. It is especially efficient for processing multiple high-resolution images in context.

**Multi-modal LLM with MMFS.** The input of multi-modal LLMs is an interleaved sequence of image and text token embeddings, which always starts with a special token  $\langle s \rangle$  and ends with another special token  $\langle /s \rangle$ . Image token embeddings are inserted at the corresponding positions in the original sequence. Another special token  $\langle \text{BoI} \rangle$  is added in front of each image to represent ‘‘Begin of Image’’.

MMFS modules are inserted between the self-attention layer and the feed-forward layer of the LLM every fixed number of blocks. Query token  $f_q$  iterates over each token in the LLM, which can only access the previous images.  $\hat{p}_q = (0.5, 0.5)$ . The output of MMFS is multiplied by  $\tanh(\alpha)$  before being added back to  $f_q$ , where  $\alpha$  is a zero-initialized learnable scalar.

**Image Decoder with MMFS.** The output features from the multi-modal LLM are further processed by another Perceiver Resampler before being fed into the image decoder. For each image to be generated, the Resampler maps previous context features to a fixed number of tokens (e.g., 77 tokens) to match the pre-trained diffusion model.

MMFS modules are inserted after each upsampling block in the U-Net structure of the diffusion model. Query token  $f_q$  iterates over each pixel in the feature map.  $\hat{p}_q$  is set as the spatial coordinate of the query pixel. The output of MMFS is further processed by a zero-initialized convolution layer before being added back to  $f_q$ .

**Training Target and Inference Pipeline.** The training objective is defined as the sum of Next-Text-Token Prediction loss in Eq. (2) and Next-Image Prediction loss in Eq. (3),

$$\mathcal{L} = \mathcal{L}_{NTP} + \lambda \mathcal{L}_{NIP} \tag{5}$$

where  $\lambda$  is a hyperparameter used to determine the relative loss weight between the image and text decoding branches. The whole framework can be optimized end-to-end.

During inference, the images and texts are generated in an auto-regressive manner. Text tokens are sampled from the distribution predicted by the multi-modal LLM. When the generated token is  $\langle \text{BoI} \rangle$ , the diffusion model is called for generating the next image.

## 4. Experiment

### 4.1. Implementation Details

**Network.** We adopt CLIP-ViT-L/14 [70], Vicuna-13B [105] and Stable Diffusion v2.1 [74] as the image encoder, large language model, and image decoder, respectively. For the multi-modal LLM, a Perceiver Resampler with 12 blocks is used to reduce the number of visual tokens per image to 64. The MMFS module is inserted every 4 blocks in the LLM. For the image decoder, a Perceiver Resampler with only 1 block is used to reduce the number of conditional tokens per image to 77. The MMFS module is inserted after each up-sampling block in the image decoder.

Method	LLM	H I A	COCO	Flickr	NoCaps	I2Para.	VQA <sup>v2</sup>	OKVQA	GQA	VizWiz	TextVQA	VisDial
Models for Text-Generation Only												
MetaLM [30]	MetaLM	- - -	82.2	43.3	58.7	-	41.1	11.4	-	41.1	11.4	-
OF-9B [5]	MPT-7B	- - -	79.5	59.5	-	-	52.7	37.8	-	27.5	24.2	-
IDEFICS-80B [36]	LLaMA-65B	- - -	91.8	53.7	65.0	-	60.0	-	45.2	36.0	30.9	-
KOSMOS-1 [33]	MetaLM	H - -	-	65.2	-	-	46.7	-	-	-	-	-
KOSMOS-2 [67]	KOSMOS-1	H - -	-	66.7	-	-	45.6	-	-	-	-	-
Flamingo-9B [3]	Chinchilla-7B	H - -	79.4	61.5	-	-	51.8	44.7	-	28.8	31.8	48.0
Flamingo-80B [3]	Chinchilla-70B	H - -	84.3	67.2	-	-	56.3	50.6	-	31.6	35.0	52.0
IDEFICS-80B-1 [36]	LLaMA-65B	- I -	117.2	65.3	104.5	-	37.4	-	-	26.0	-	-
mPLUG-DocOwl [95]	LLaMA-7B	- I A	52.6	62.2	57.4	-	-	-	-	-	-	-
BLIP-2 [48]	Vicuna-7B	- I A	-	74.9	107.5	-	-	-	38.6	25.3	40.1	-
BLIP-2 [48]	Vicuna-13B	- I A	-	71.6	103.9	-	41.0	-	41.0	19.6	42.5	-
InstructBLIP [14]	Vicuna-7B	- I A	-	82.4	123.1	-	-	-	49.2	34.5	50.1	-
InstructBLIP [14]	Vicuna-13B	- I A	-	82.8	121.9	-	-	-	49.5	33.4	50.7	-
Shikra [10]	Vicuna-13B	- I A	117.5	73.9	-	-	77.4	-	-	-	-	-
LLaVA-1.5 [52]	Vicuna-7B	- I A	-	-	-	-	78.5	-	62.0	50.0	58.2	-
LLaVA-1.5 [52]	Vicuna-13B	- I A	-	-	-	-	80.0	-	63.3	53.6	61.3	-
VL-GPT-I [108]	LLaMA-7B	- I A	133.7	-	-	-	67.2	50.3	51.5	38.9	-	51.8
Qwen-VL [6]	Qwen-7B	H I A	-	85.8	121.4	-	78.8	-	59.3	35.2	63.8	-
Qwen-VL-Chat [6]	Qwen-7B	H I A	-	81.0	120.2	-	78.2	-	57.5	38.9	61.5	-
Models for both Image and Text Generation												
CM3Leon [99]	-	H - -	61.6	-	-	10.5	47.6	23.8	-	37.6	-	22.6
Emu [83]	Vicuna-13B	H - -	112.4	-	-	-	52.0	38.2	-	34.2	-	47.4
Emu-I [83]	Vicuna-13B	H - -	117.7	-	-	-	40.0	34.7	-	35.4	-	48.0
Emu2 [81]	LLaMA-33B	H - -	-	-	-	-	33.3	26.7	-	40.4	26.2	-
DreamLLM [18]	Vicuna-7B	- I -	115.4	-	-	17.4	56.6	44.3	-	38.1	34.9	-
VL-GPT [108]	LLaMA-7B	- - -	116.4	-	-	-	51.7	35.8	34.6	34.7	-	49.9
MM-Interleaved	Vicuna-13B	- - -	129.0	85.8	106.4	23.5	57.0	40.0	-	40.8	37.2	48.7
MM-Interleaved-SFT	Vicuna-13B	- I A	140.5	93.0	123.2	30.3	80.2	51.7	60.5	54.9	61.0	53.7

Table 1. **Multi-modal comprehension evaluation.** ‘H’ denotes using in-house data, ‘I’ means the training images of some benchmarks are included in the training, ‘A’ means the training annotations of some benchmarks are visible in training. Some benchmark names are abbreviated due to space limits. COCO [11]; Flickr: Flickr30k [68]; NoCaps [2]; I2Para.: Image2Paragraph [44]; VQA<sup>v2</sup>: VQAv2 [27]; OKVQA [59]; GQA [35]; VizWiz [29]; TextVQA [80]; VisDial [15].

**Pre-training.** Our models are pre-trained on a mixture of interleaved image-text sequences and image-text pairs, including MMC4 [109], LAION-2B [76], LAION-COCO [77], CC-12M [8] and Objects365 [78]. For CC-12M [8] and Objects365 [78], instead of utilizing the original annotations, we use the pre-trained BLIP-2 model [48] to caption the images. The sampling probability of MMC4 is twice that of other image-text pair datasets. No in-house data is used.

The images are inserted before or after the corresponding text sentence with equal probability. To optimize training efficiency and data utility, multiple image-text pairs or interleaved image-text sequences are concatenated into extended sequences with the maximum context length (*i.e.*, 2,048 tokens).

The model is pre-trained for 15,000 steps with 11 billion tokens visited. The image encoder and LLM are frozen. The learning rate is set to be  $10^{-5}$  for the image decoder and  $10^{-4}$  for the rest trainable parameters. The input and output image resolutions are  $224 \times 224$  and  $512 \times 512$ , respectively.

**Supervised Fine-tuning.** After pre-training, like multi-modal LLMs, our model capabilities can be further enhanced using supervised fine-tuning. The model is fine-

tuned on four types of downstream tasks, which are 1) visual question-answering and image caption, 2) referring expression comprehension, 3) segmentation-to-image translation, and 4) visual storytelling.

More details of datasets and hyper-parameters used for pre-training and fine-tuning could be found in the Appendix.

## 4.2. Evaluation

We evaluate the zero-shot visual-language capability of the pre-trained MM-Interleaved as well as its performance on various downstream tasks after fine-tuning and report the results in Tab. 1.

**Zero-shot Results after Pre-training.** Our method demonstrates strong multi-modal zero-shot comprehension on various benchmarks, including image captioning on COCO [11], Flickr30K [68], NoCaps [2] and Image2Paragraph [44]; general visual question answering on VQAv2 [27], OKVQA [59], VizWiz [29] and TextVQA [80]. We also evaluate on the VisDial [15] visual dialogue task. In the fully decontaminated setting where the image and text in downstream tasks are unseen during pre-training, our model significantly outperforms MetaLM [30],

Model	RefCOCO [42]			RefCOCO+ [58]			RefCOCOg [58]	
	Val	Test-A	Test-B	Val	Test-A	Test-B	Val	Test
OFA-L [88]	79.96	83.67	76.39	68.29	76.00	61.75	67.57	67.50
VisionLLM-H [90]	-	86.70	-	-	-	-	-	-
Shikra [10]	87.01	90.61	80.24	81.60	87.36	72.12	82.27	82.19
MiniGPT-V2 [9]	88.69	91.65	85.33	79.97	85.12	74.45	84.44	84.66
Ferret [96]	<b>89.48</b>	<b>92.41</b>	84.36	<b>82.81</b>	<b>88.14</b>	75.17	<b>85.83</b>	<b>86.34</b>
* Qwen-VL [6]	<b>89.36</b>	<b>92.26</b>	85.34	<b>83.12</b>	<b>88.25</b>	<b>77.21</b>	<b>85.58</b>	85.48
MM-Interleaved (ours)	<b>89.92</b>	<b>92.59</b>	<b>86.54</b>	<b>82.99</b>	<b>88.57</b>	<b>77.07</b>	<b>85.21</b>	84.92

Table 2. **Supervised fine-tuning results on referring expression comprehension task.** “\*” denotes using an additional self-constructed grounding dataset and trained with an image resolution larger than 224.

Model	MS-COCO	LN-COCO
Text-to-Image Specialists		
Retrieval Result	17.97	33.59
DALL-E [71]	~28	-
CogView [16]	27.10	-
CogView2 [17]	24.00	-
Stable Diffusion [74]	12.43	34.26
GLIDE [63]	12.24	-
Make-A-Scene [25]	11.84	-
DALL-E 2 [72]	10.39	-
Muse-3B [94]	7.88	-
Imagen-3.4B [75]	7.27	-
Parti-20B [98]	7.23	15.97
Models for both Image and Text Generation		
CM3-13B [1]	29.56	-
VL-GPT [108]	12.25	-
GILL [43]	12.20	-
Emu-13B [83]	11.66	-
CM3Leon-7B [99]	10.82	-
DreamLLM-7B-Stage1 [18]	8.76	22.42
DreamLLM-7B [18]	8.46	20.53
MM-Interleaved-13B (ours)	7.90	23.88

Table 3. **Zero-shot text-to-image generation** results on MS-COCO [51] and LN-COCO [69]. FID [31] is reported.

OF-9B [5] and IDEFICS-80B [45] on all captioning, VQA, and multi-modal tasks. This demonstrates the effectiveness of the proposed MM-Interleaved approach. Furthermore, our model even exceeds most trained on vast in-house data like Flamingo-9B [3] and Emu [83], showing the importance of proper architecture for image-text interaction.

Additionally, we evaluate text-conditional image generation on MS-COCO [51] and LN-COCO [69]. On MS-COCO, we sample 8 images per text condition and use CLIP [70] to rerank based on text-image similarity. CLIP reranking is not used for LN-COCO. FID [31] is used to evaluate both datasets. As show in Tab. 3, our model shows competitive text-to-image generation compared to existing image and text generation models.

**Fine-tuning Results of VQA and Captioning.** Our fine-tuned model achieves state-of-the-art performance on image captioning benchmarks. On visual question answering tasks, it matches the previous best LLaVA-1.5 model [52]. Compared to LLaVA-1.5, our model has two key advan-

tages 1) our method is capable of generating both images and text, while LLaVA-1.5 can only generate text; 2) LLaVA-1.5 uses 576 visual tokens as LM inputs, whereas we only require 64. Our model achieves competitive image understanding with far fewer visual tokens, making it better suited for multi-image scenarios.

**Fine-tuning Results of Referring Expression Comprehension.** Our model demonstrates state-of-the-art performance on various referring expression comprehension (REC) benchmarks, as shown in Tab. 2. Compared to recent REC models like VisionLLM [90] and Shikra [10], our model outperforms on most datasets. Remarkably, even though we only use public REC data [42, 58] for fine-tuning, our model matches QWen-VL [6] which utilizes an extra 22M in-house grounding dataset and trains at higher resolution (448 vs 224 pixels). This shows the effectiveness of synchronized fine-grained image features for enhancing the REC capability of our model.

**Fine-tuning Results of Segmentation-to-Image Translation.** We follow the protocol proposed in ControlNet [100] by generating images from ADE20K ground truth semantic masks and use OneFormer [38] for segmenting the generated images. Standard mIoU is reported as a metric for measuring the semantic and structural fidelity of the generated images. We show the results in Tab. 4a. MM-Interleaved clearly outperforms other baselines including ControlNet by a large margin. Compared to ControlNet, our model could leverage the better representations learned by our generative modeling from large-scale pre-training data, which benefits the image generation tasks. Moreover, thanks to MMFS, our model is capable of generating realistic images with pixel-level precise alignment from a semantic label map, where simply relying on coarse Perceiver Resampler features fails on this task, which we will show in the ablation studies.

**Fine-tuning Results of Visual Storytelling.** Besides text-to-image and image-to-image generation, our MM-Interleaved could also condition on interleaved image-text as context for generating new images. We evaluate our model’s performance both for generating the last image on the Visual StoryTelling (VIST) dataset [34] and for generat-

ADE20K (GT) [38]	VQGAN [20]	LDM [73]
0.58	0.21	0.31
PIPT [89]	ControlNet [100]	Ours
0.26	0.35	<b>0.44</b>

(a) Segmentation-to-image generation results on ADE20K [106] mIoU ( $\uparrow$ ) is reported.

Method	CLIP Sim. $\uparrow$	FID $\downarrow$
GILL [43]	0.64	-
MiniGPT-5 [104]	<b>0.70</b>	59.5
MM-Interleaved	<b>0.70</b>	<b>39.7</b>

(b) Image generation results on VIST [34].

Model	Pororo	Flintstones
StoryDALL-E [57]	25.9	26.5
AR-LDM [66]	17.4	19.3
ACM-VSG [23]	15.4	<b>18.4</b>
MM-Interleaved	<b>14.7</b>	<b>18.7</b>

(c) Autoregressive image generation results on Pororo [49] and FlintStones [28]. FIDs( $\downarrow$ ) are reported.

Table 4. **Comparative analysis of image generation ability of MM-Interleaved.**

ing multiple images autoregressively on the Pororo [49] and Flintstones [28] datasets. As is shown in Tab. 4b and 4c, our model achieves SoTA performance on both CLIP-Similarity and FID metrics compared to previous works on VIST and achieves competitive performance compared with previous specialist methods on Pororo and Flintstones. More qualitative results and implementation details can be found in the appendix.

### 4.3. Ablation Study

In the ablation study, we use CLIP-ViT-L/14 [70] as the vision foundation model, OpenLLaMA-3B v2 [26] as the multi-modal LLM and miniSD<sup>1</sup> as the image decoder. The output resolution of each image is 256.

For simplicity, in this subsection, we study the effect of token efficiency, image resolution, cross-attention mechanisms, and the role of MMFS in image generation in a single-image setting, where each token only attends to the nearest preceding image. Please refer to the appendix for more detailed ablations studies in the multi-image setting.

The model is pre-trained for 10k steps on 80 NVIDIA 80G-A100 GPUs. The mini batch size of LAION-COCO [77], LAION-2B [76], and MMC4 [109] on a single GPU is 2, 2, and 4 respectively. For token efficiency, image resolution, and cross-attention mechanism, we evaluate the model’s zero-shot performance on three representative tasks and four datasets, *i.e.*, image caption on the COCO Karpathy test set, text-to-image generation on the COCO Karpathy test set, visual question answering on OKVQA [59], and TextVQA validation set. We use CIDEr, FID-5k, and top-1 accuracy as the evaluation metrics. For cross-attention in image generation, we perform supervised fine-tuning on the ADE20K [106] for the label-to-image generation task.

**Token Efficiency.** As shown in Tab. 5a, our method achieves better overall performance while only using 32 visual tokens for each input image. Such results demonstrate the effectiveness of our method when the context length is limited. To avoid the potential information bottleneck caused by the Resampler, we further increase the number of visual tokens to 256. Our method still outperforms the baseline in this setting.

**Scaling up Input Image Resolutions.** The performance gap between our method and the baseline becomes larger

when further increasing the input image resolution from 224 to 448, as shown in Tab. 5b. Such results indicate our method could better exploit the additional information gained from high resolution.

**Comparison between Different Cross Attention Mechanisms.** The ablation of adopting different cross-attention mechanisms for LLM is shown in Tab. 6. The overall performance drops when directly replacing MMFS with the vanilla dense cross attention, possibly due to its slower convergence speed on 2D data, and using a resampler performs equally well. We highlight that the model with deformable attention performs significantly better than other attention mechanisms on TextVQA, indicating that deformable attention could effectively and efficiently capture fine-grained information like text needed for the task, such as visual question answering in this case.

**MMFS for Image Generation.** We study whether adding MMFS is critical for image generation on the segmentation-to-image task. This task is hard as it requires precious pixel-level information to align the given segmentation condition and image output properly. From the results in Tab. 5c, it is clear that the model without MMFS failed to generate images spatially aligned with the segmentation image condition, showing extremely low mIoU results. We show visualizations of the generated results in the supplementary material to provide a visual comparison. It is worth noting that the quality of the generated image from the model without MMFS is still high and properly aligned with the text description input; however, without MMFS, the model cannot preserve all spatial information, and the spatial alignment for the generated results is poor.

## 5. Conclusion

In conclusion, this paper presented MM-Interleaved, an end-to-end generative model specifically designed for interleaved image-text data. The unique contribution of MM-Interleaved lies in the novel multi-scale and multi-image feature synchronizer module, which significantly enhances the model’s capability to access and integrate fine-grained image features. This design addresses the longstanding limitation in existing models where a fixed number of visual tokens inadequately capture intricate image details, especially in scenarios involving multiple images. Pre-trained on diverse image-text datasets and further refined through

<sup>1</sup><https://huggingface.co/justinpinkney/miniSD>

# Token	w/ MMFS	Caption $\uparrow$	Generation $\downarrow$	OK-VQA $\uparrow$	TextVQA $\uparrow$
32		107.0	32.2	28.7	22.5
32	✓	<b>110.6</b>	<b>30.0</b>	<b>29.8</b>	<b>27.7</b>
256		<b>110.7</b>	32.7	29.2	23.6
256	✓	<b>110.9</b>	<b>29.5</b>	<b>29.6</b>	<b>27.8</b>

(a) pre-training with 224 input resolution

w/ MMFS	Caption $\uparrow$	Generation $\downarrow$	OK-VQA $\uparrow$	TextVQA $\uparrow$
	110.5	<b>30.3</b>	29.9	24.9
✓	<b>115.2</b>	<b>30.5</b>	<b>30.6</b>	<b>30.8</b>

(b) fine-tuning with 448 input resolution

w/ MMFS	ADE20k $\uparrow$
	5.3
✓	<b>35.9</b>

(c) fine-tuning for image translation

Table 5. **Ablation on the usage of MMFS module.** “Genetation” is the text-to-image generation task. “ADE20k” is the segmentation-to-image translation task. Others are text generation tasks. “# Token” indicates the number of input visual tokens for LLM (32 by default).

Cross-Attn	Transition	Attn Input	COCO Cap. $\uparrow$	COCO Gen. $\downarrow$	OK-VQA $\uparrow$	TextVQA $\uparrow$
Deformable	None	16 $\times$ 16	<b>110.6</b>	<b>30.0</b>	<b>29.8</b>	<b>27.7</b>
Dense	None	16 $\times$ 16	108.5	30.6	28.4	23.6
Dense	Resampler	32 tokens	107.2	30.7	28.9	24.0

Table 6. **Ablation on the design choice of MMFS module.** Different attention modules can be used in MMFS. We also ablate whether to add additional transition layer before feeding image features into MMFS. Transformer attention with Resampler transition on single scale and single image is similar to the cross attention used in Flamingo. “Self-Attention” has the same parameters with “Resampler”.

supervised fine-tuning, MM-Interleaved shows a respectful proficiency in processing complex multi-modal instructions. The empirical results modestly highlight its ability to discern intricate visual details and generate images that align accurately with both textual and visual inputs.

## A. Additional Ablation Studies

This section provides more ablation studies for MM-Interleaved, all of which share the same settings as those in the main text by default. Note that these models are not fine-tuned on downstream tasks.

**Pre-training with Different Loss Terms.** As showed in Tab. 7, MM-Interleaved achieves better performance when jointly trained with both  $\mathcal{L}_{NTP}$  and  $\mathcal{L}_{NIP}$  on comprehension and generation tasks, demonstrating the mutual benefits between the two loss terms. Moreover, setting  $\lambda = 10$  achieves a better balance between  $\mathcal{L}_{NTP}$  and  $\mathcal{L}_{NIP}$  empirically.

Loss Term	Caption $\uparrow$	Generation $\downarrow$	OK-VQA $\uparrow$	TextVQA $\uparrow$
$\mathcal{L}_{NTP} + 100 \mathcal{L}_{NIP}$	106.2	31.1	<b>29.8</b>	24.5
$\mathcal{L}_{NTP} + 10 \mathcal{L}_{NIP}$	<b>110.6</b>	<b>30.0</b>	<b>29.8</b>	<b>27.7</b>
$\mathcal{L}_{NTP} + \mathcal{L}_{NIP}$	<b>110.0</b>	31.4	29.3	26.0
$\mathcal{L}_{NTP}$ only	105.7	–	<b>29.9</b>	<b>27.6</b>
$\mathcal{L}_{NIP}$ only	–	34.2	–	–

Table 7. Pre-training with different loss terms.

**The Relationship between MMFS and resampler.** The results in Tab. 8 validate the mutual benefits between our proposed MMFS module and the Resampler used in image tokenizer, as removing either of them leads to an overall performance degradation.

w/ Resampler	w/ MMFS	Caption $\uparrow$	Generation $\downarrow$	OK-VQA $\uparrow$	TextVQA $\uparrow$
✓	✓	<b>110.6</b>	<b>30.0</b>	<b>29.8</b>	<b>27.7</b>
✓		107.0	32.2	28.7	22.5
	✓	102.7	32.0	27.3	22.0

Table 8. The complementary relationship between MMFS and Resampler. When not using Resampler, we directly feed 32 randomly-initialized learnable embeddings as input visual tokens into the LLM.

**MMFS with Multi-Image and Multi-Scale.** As shown in Tab. 9, adding multi-image and multi-scale for MMFS improves the model’s performance on VQA tasks. To better take advantage of the multi-image mechanism, we follow [3, 83] to further evaluate our model with few-shot prompts. Two training samples including both image and text are selected as the input prompts. The results in Tab. 10 demonstrates that MMFS with multi-image and multi-scale benefits the most from the few-shot setting, indicating its potential capability for interleaved image-text modeling.

multi-scale	multi-image	Caption $\uparrow$	Generation $\downarrow$	OK-VQA $\uparrow$	TextVQA $\uparrow$
		110.6	30.0	29.8	27.7
✓		111.2	29.5	30.3	28.1
✓	✓	111.2	29.9	31.1	28.2
<i>finetuning with 448 input resolution</i>					
		115.2	30.5	30.6	30.8
✓		115.4	30.1	31.0	31.3
✓	✓	115.8	30.0	31.7	32.0

Table 9. Zero-shot evaluation results of MMFS.

multi-scale	multi-image	OK-VQA $\uparrow$	TextVQA $\uparrow$
		36.5	30.7
✓		38.5	31.1
✓	✓	38.7	33.1
<i>finetuning with 448 input resolution</i>			
		38.3	36.6
✓		38.7	37.7
✓	✓	39.1	37.9

Table 10. 2-shot evaluation results of MMFS on VQA tasks.

## B. Implementation Details

### B.1. Pre-training

**Dataset Details.** We use MMC4 [109], LAION-2B, LAION-COCO [77], CC-12M [8] and Objects365 [78] as the pre-training dataset. LAION-2B is the English subset of LAION-5B [76], and we further filter it based on additional metrics including aesthetics scores. LAION-COCO [77] is a 600M subset of LAION-2B, which is captioned by pre-trained BLIP [47] models. Text prompts with length shorter than 10 are also filtered out. For CC-12M [8] and Objects365 [78], instead of utilizing the original annotations, we use the pre-trained BLIP-2 model [48] to caption the images. Following previous works [18, 83], additional filtering rules are applied to the MMC4 dataset [109]. Specifically, images with a CLIP similarity score below 0.24 will be discarded, and only 6 images at most will be kept for each document. We also exclude 100% of all documents that do not contain any images, and 50% of documents that contain only 1 image.

**Data Concatenation Strategy.** For image-text-pair datasets (e.g., LAION-2B, LAION-COCO [77]), we randomly sample multiple image-text pairs from the same dataset and concatenate them to the maximum context length (i.e., 2048) during pre-training. For interleaved image and text datasets (i.e., MMC4 [109]), we also split and concatenate the documents to form the training samples. Such concatenation strategy can utilize the full context window of Large Language Models and thus achieve high data efficiency.

**More Training Details .** The detailed hyper-parameters of pre-training are listed in Tab. 11. Besides that, for image generation, we ignore the training loss of images which are the first element in the sequence. The text condition of the rest images are dropped with a 10% probability to improve classifier-free guidance sampling [32].

Hyper-parameters	Value
Input image resolution	224 × 224
Output image resolution	512 × 512
VFM	CLIP-ViT-L/14 (frozen)
LLM	Vicuna-13B v1.3 (frozen)
DM	Stable Diffusion v2.1
$\lambda$	10
Cross-attention frequency	4
LLM Multi-scale feature maps	$i = 2, 3, 4$
Learning rate	1e-5 (image decoder) 1e-4 (others)
Weight decay	0.05
Warmup steps	1k
Learning rate schedule	cosine with warmup
Training iterations	15k
Context length	2048
Optimizer	AdamW
Optimizer hyper-parameters	$\beta_1, \beta_2, \epsilon = 0.9, 0.995, 1e-6$
Data	MMC4, LAION-2B, LAION-COCO, CC-12M, Objects365
Augmentation	CenterCrop
Batch size (per GPU)	2,2,4

Table 11. Hyper-parameters for pre-training.

### B.2. Supervised Fine-tuning

**VQA and Image Captioning.** For this task, we train our model in the form of question answering, i.e., using `Based on the image, please answer the question. {image}{question}. The answer is: {answer}` as the instruction prompt. We utilize public available datasets for supervised fine-tuning, including LLaVA-Mix-665K [52], COCO Caption [11], VQAv2 [27], ChartQA [60], DocVQA [13], EST-VQA [92], InfoVQA [61], STVQA [92], TextCaps [79], LLaVAR [102], OCR-VQA [62], and DVQA [41]. See Tab. 12 for more training details.

Hyper-parameters	Value
Input image resolution	448 × 448
Learning rate	1e-6 (language model) 1e-5 (others)
Weight decay	0.05
Warmup steps	500
Learning rate schedule	cosine
Training iterations	10k
Optimizer	AdamW
Optimizer hyper-parameters	$\beta_1, \beta_2, \epsilon = 0.9, 0.999, 1e-8$
Batch size	256

Table 12. Hyper-parameters for VQA and image captioning.

**Referring Expression Comprehension.** Following previous works [6, 10], we train our model in the form of VQA, i.e., the prompt being `Question: Provide the bounding box coordinate of the region this sentence describes: {object}, Answer: (x1,y1)(x2,y2)`. The generated bounding box is considered correct if its intersection over union (IoU) with the GT box is greater than 0.5. Only public available datasets, including datasets from RefCOCO [42], RefCOCO+ [58], and RefCOCOg [58] are utilized to train MM-Interleaved. See Tab. 13 for fine-tuning hyper-parameters.

Hyper-parameters	Value
Input image resolution	224 × 224
Learning rate	2e-5
Weight decay	0.05
Warmup steps	500
Learning rate schedule	cosine
Training iterations	10k
Optimizer	AdamW
Optimizer hyper-parameters	$\beta_1, \beta_2, \epsilon = 0.9, 0.999, 1e-8$
Augmentation	RandomHorizontalFlip
Batch size	256

Table 13. Hyper-parameters for referring expression comprehension.

**Segmentation-to-Image Translation.** Following ControlNet [100], we use BLIP [47] to generate text captions for each image in the ADE20K dataset. We train our model on the training set and evaluate on the validation set. The input sequence is formulated as  $\{\text{segmentation image}\}\{\text{caption}\}\{\text{ground truth image}\}$  for each segmentation-image pair. See Tab. 14 for more training details.

Hyper-parameters	ADE20K
Input image resolution	$224 \times 224$
Output image resolution	$512 \times 512$
Learning rate	1e-5 (image decoder) 1e-4 (others)
Weight decay	0.05
Warmup steps	100
Learning rate schedule	cosine
Training iterations	4k
Optimizer	AdamW
Optimizer hyper-parameters	$\beta_1, \beta_2, \epsilon = 0.9, 0.98, 1e-5$
Augmentation	RandomHorizontalFlip
Batch size	512

Table 14. Hyper-parameters for Segmentation-to-Image Translation.

**Visual Storytelling.** Following previous works [43, 66, 104], MM-Interleaved is finetuned on the following three visual storytelling datasets respectively:

- **VIST** [34] is a real-world vision-language dataset, containing 34k and 5k samples for training and evaluation. Each sample is a sequence consisting of 5 text captions and images. During training, we concatenate all the texts and images sequentially and the model is trained to predict all images. During inference, we test the model on generating the last image in the sequence, conditioned on all preceding images and texts following [43, 104]. The evaluation metrics are FID [31] and the CLIP similarity [70] between the generated images and the corresponding real images.
- **PororoSV** [49] and **FlintstonesSV** [56] are two cartoon storytelling datasets, containing 10191/2334/2208 and 20132/2071/2309 samples of the train, validation, and test set, respectively. Each sample is a sequence consisting of 5 text captions and frame images. During training, all the texts and images are concatenated sequentially and the model is trained to predict all images. During inference, the last 4 images are generated auto-regressively given the first image and all preceding captions as condition. FID [31] is used as the evaluation metric.

The finetuning hyper-parameters are listed in Tab. 15.

Hyper-parameters	VIST / PororoSV / FlintstonesSV
Input image resolution	$224 \times 224$
Output image resolution	$512 \times 512$
Learning rate	1e-4 (image decoder) 1e-5 (others)
Weight decay	0.05
Warmup steps	200
Learning rate schedule	cosine
Training iterations	4k
Optimizer	AdamW
Optimizer hyper-parameters	$\beta_1, \beta_2, \epsilon = 0.9, 0.98, 1e-8$
Augmentation	CenterCrop
Batch size	128

Table 15. Hyper-parameters for visual storytelling.

### B.3. Evaluation

**Benchmarks.** Evaluating MM-Interleaved comprehensively requires various benchmarks and datasets, such as image caption, visual question answering, text-to-image generation and so on. All these evaluation tasks and metrics are listed in Tab. 16.

**Image Generation.** For all image generation tasks, the scale of classifier-free guidance [32] and the total inference step is set as 3.5 and 250 by default.

**Text Generation.** The prompt templates for each text generation tasks are listed in Tab. 17. The ‘Image Caption (short)’ task includes COCO Caption [11], Flickr30k [68] and NoCaps [2], while the ‘Image Caption (long)’ task includes Image2Paragraph [44].

## C. Qualitative Results

### C.1. VL Comprehension

**Text Reading QA.** As is shown in Fig. 5, MM-Interleaved with MMFS provides more accurate answers when requiring fine-grained details for generating text outputs given VL inputs.

**Referring Expression Comprehension.** The visualization of MM-Interleaved on REC tasks is shown in Fig. 6. Our model with MMFS is also capable of generating more accurate coordinates given the referring expression and the query image.

### C.2. Image Generation

**Segmentation-to-image Translation.** Fig. 7 shows the visualization results of MM-Interleaved for segmentation-to-image translation. Given the text prompt and segmentation map, the spatial layout of images generated with MMFS is significantly closer to the original ground-truth image, compared to the baseline results without MMFS.

**Multi-image Generation.** In Fig. 8, we compare the multiple images sequentially generated by MM-Interleaved with

	Dataset	Task	Split	Metric
Caption.	COCO [11]	Scene description	test	CIDEr(↑) [87]
	Flickr30k [68]	Scene description	test	CIDEr(↑) [87]
	NoCaps [2]	Scene description	test	CIDEr(↑) [87]
	Image2Paragraph [44]	Scene description	test	CIDEr(↑) [87]
VQA.	VQAv2 [27]	Scene understanding QA	test-dev	VQA Acc(↑) [4]
	OKVQA [59]	External knowledge QA	val	VQA Acc(↑) [4]
	GQA [35]	Scene understanding QA	test-dev	VQA Acc(↑) [4]
	VizWiz [29]	Scene understanding QA	test-dev	VQA Acc(↑) [4]
	TextVQA [80]	Text reading QA	val	VQA Acc(↑) [4]
	VisDial [15]	Image dialogue	val	NDCG(↑)
REC.	RefCOCO [42]	Referring experssion comprehension	-	IoU Acc(↑)
	RefCOCO+ [58]	Referring experssion comprehension	-	IoU Acc(↑)
	RefCOCOG [58]	Referring experssion comprehension	-	IoU Acc(↑)
Generation.	MS-COCO [51]	Text-to-image generation	val-30K	FID(↓) [31]
	LN-COCO [69]	Text-to-image generation	val-30k	FID(↓) [31]
	ADE20k [106]	Segmentation-to-image generation	val	mIoU(↑)
	VIST [34]	Interleaved-context image generation	val	CLIP-Sim(↑) [70], FID(↓) [31]
	PororoSV [49]	Interleaved-context multi-image generation	test	FID(↓) [31]
	FlintstonesSV [28]	Interleaved-context multi-image generation	test	FID(↓) [31]

Table 16. Summary of evaluation benchmarks, including image caption, visual question answering, referring experssion comprehension, and image generation.

	Task	Prompt Template
Zero-shot	Image Caption (short)	{image} a photo of
	Image Caption (long)	{image} Please describe the image in detail. The image depicts
	VQA (except VizWiz)	Based on the image, please answer the question. {image}{question} Please provide an accurate answer within one word. The answer is:
	VizWiz QA	Based on the image, please answer the question. {image}{question} When the provided information is insufficient, respond with 'Unanswerable'. Please provide an accurate answer within one word. The answer is:
	Visual Dialog	{image} caption: {caption} question: {history question}? answer: {history answer}. ... question: {question}? answer:
Supervised Fine-tuning	Image Caption (short)	{image} Provide a one-sentence caption for the provided image.
	Image Caption (long)	{image} Please describe the image in detail.
	VQA (except VizWiz)	Based on the image, please answer the question. {image}{question} Please provide an accurate answer within one word. The answer is:
	VizWiz VQA	Based on the image, please answer the question. {image}{question} When the provided information is insufficient, respond with 'Unanswerable'. Please provide an accurate answer within one word. The answer is:
	Visual Dialog	{image} caption: {caption} question: {history question}? answer: {history answer}. ... question: {question}? answer:

Table 17. Prompt templates for text generation.



User: what year is written on the bottom?

MM-Interleaved (w. MMFS): 2011.

MM-Interleaved (w/o MMFS): 2022.



User: what is in the bottles?

MM-Interleaved (w. MMFS): Corona.

MM-Interleaved (w/o MMFS): Tequila.



User: what is the number of the player at bat?

MM-Interleaved (w. MMFS): 79.

MM-Interleaved (w/o MMFS): 9.



User: what brand is on the middle shelf?

MM-Interleaved (w. MMFS): Coke.

MM-Interleaved (w/o MMFS): Pepsi.



User: how many stars can you see on the white board?

MM-Interleaved (w. MMFS): 3.

MM-Interleaved (w/o MMFS): 5.



User: what brand is represented here?

MM-Interleaved (w. MMFS): Intel.

MM-Interleaved (w/o MMFS): Dell.

Figure 5. **Qualitative results on TextVQA [80]**. Each example consists of the user query, the answer given by MM-Interleaved with *MMFS*, and the answer given by MM-Interleaved without *MMFS*. The image shapes are normalized for visualization.



User: a sweet foo in an orange bowl

MM-Interleaved (w. MMFS): (595,090)(855,520)

MM-Interleaved (w/o MMFS): (595,507)(892,981)



User: a laptop

MM-Interleaved (w. MMFS): (581,001)(999,989)

MM-Interleaved (w/o MMFS): (336,170)(619,754)



User: an orange bus in between two other buses

MM-Interleaved (w. MMFS): (619,507)(892,792)

MM-Interleaved (w/o MMFS): (482,514)(634,790)



User: part of a small white airplane with three windows

MM-Interleaved (w. MMFS): (000,316)(418,599)

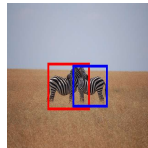
MM-Interleaved (w/o MMFS): (000,000)(997,707)



User: a head of broccoli sits on the table

MM-Interleaved (w. MMFS): (000,569)(242,984)

MM-Interleaved (w/o MMFS): (000,000)(402,627)



User: zebra with its head behind the other zebra

MM-Interleaved (w. MMFS): (276,406)(563,727)

MM-Interleaved (w/o MMFS): (446,422)(684,709)

Figure 6. **Referring Expression Comprehension on RefCOCOg [58]**. Each example consists of the user query, the box predicted with *MMFS*, and the box predicted without *MMFS*. The image shapes are normalized for visualization.

and without MMFS. The images generated with MMFS achieves better spatial consistency (*e.g.* the background environment, change of viewpoint, character position relationship *etc.*) and closer semantic alignment with the interleaved image-text context.

**Generating Interleaved Image and Texts.** Moreover, the

model is further finetuned to generate both images and texts simultaneously for visual storytelling tasks. As is shown in Fig. 9, given the first frame image and caption as context, MM-Interleaved with MMFS generates the following interleaved images and texts coherently, achieving balance between the generation diversity and spatial semantic con-

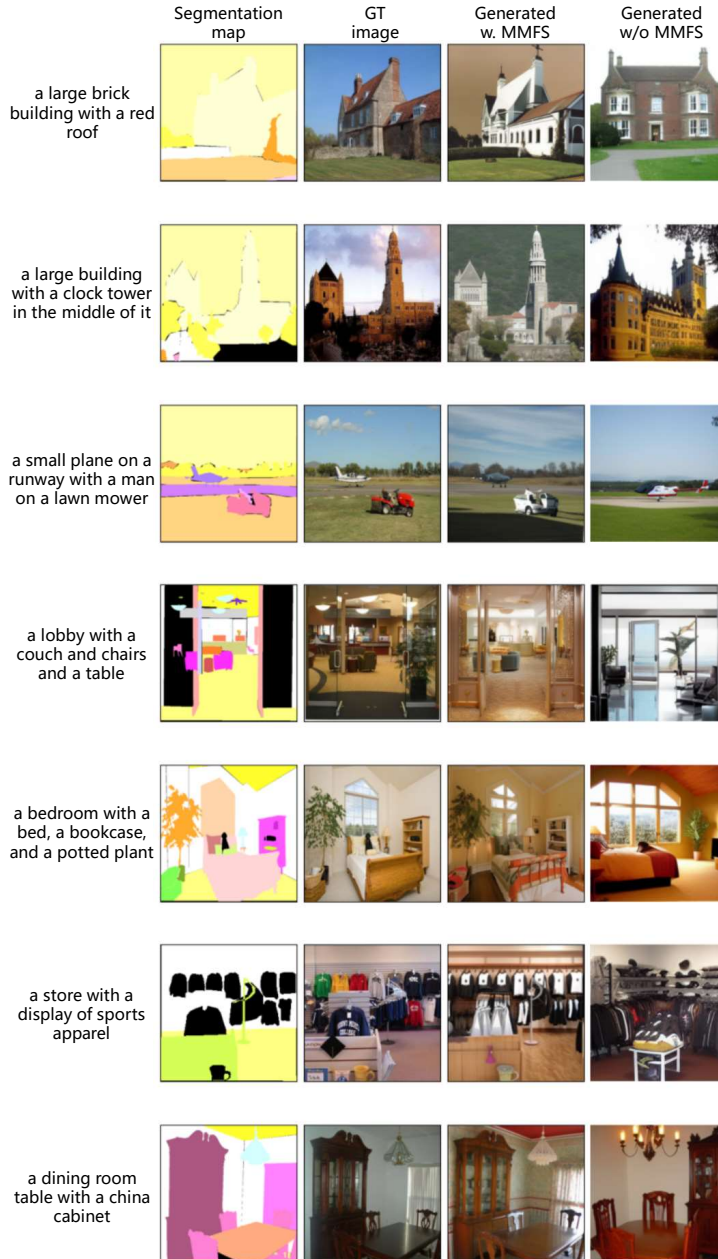


Figure 7. **Segmentation-to-Image Generation on ADE20k [106]**. Each row is an example consisting of four images, which are the input segmentation map, the ground truth image, the generated image *with MMFS*, and the generated image *without MMFS* respectively. The shape of ground-truth images and segmentation maps is normalized for visualization. When *without MMFS*, the generated results lack spatial alignment with the input segmentation maps.

sistency.

## D. Future Work

Future works of MM-Interleaved aims to further scale up both the model and data size, enabling end-to-end training with full-parameters from scratch. In addition, we believe that it is also worth exploring to build a comprehensive evaluation benchmark specifically designed for interleaved

image-text modeling.

## References

- [1] Armen Aghajanyan, Bernie Huang, Candace Ross, Vladimir Karpukhin, Hu Xu, Naman Goyal, Dmytro Okhonko, Mandar Joshi, Gargi Ghosh, Mike Lewis, et al. Cm3: A causal masked multimodal model of the internet. *arXiv preprint arXiv:2201.07520*, 2022. 7
- [2] Harsh Agrawal, Karan Desai, Yufei Wang, Xinlei Chen,



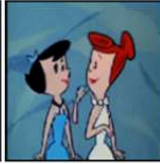
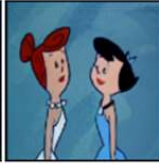
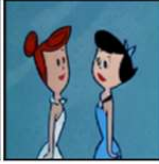
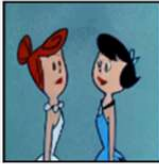
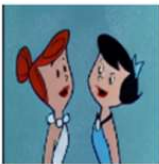
Figure 8. **Multi-image Generation on PororoSV [49] and FlintstonesSV [28]**. Each example consists of four rows. The first row is the first frame image and all corresponding captions. The second row contains the ground truth images of following frames; The third row are the generated results *with MMFS*; And the last row are the results generated *without MMFS*. When *without MMFS*, the generated multiple images lack content consistency in terms of characters, backgrounds, objects, etc.

Rishabh Jain, Mark Johnson, Dhruv Batra, Devi Parikh, Stefan Lee, and Peter Anderson. Nocaps: Novel object captioning at scale. In *ICCV*, 2019. 6, 11, 12

- [3] Jean-Baptiste Alayrac, Jeff Donahue, Pauline Luc, Antoine Miech, Iain Barr, Yana Hasson, Karel Lenc, Arthur Mensch, Katherine Millican, Malcolm Reynolds, et al. Flamingo: a visual language model for few-shot learning. *NeurIPS*, 2022. 2, 3, 4, 6, 7, 9
- [4] Stanislaw Antol, Aishwarya Agrawal, Jiasen Lu, Margaret Mitchell, Dhruv Batra, C. Lawrence Zitnick, and Devi Parikh. VQA: visual question answering. In *ICCV*, 2015. 12
- [5] Anas Awadalla, Irena Gao, Josh Gardner, Jack Hessel, Yusuf Hanafy, Wanrong Zhu, Kalyani Marathe, Yonatan

Bitton, Samir Gadre, Shiori Sagawa, et al. Openflamingo: An open-source framework for training large autoregressive vision-language models. *arXiv preprint arXiv:2308.01390*, 2023. 6, 7

- [6] Jinze Bai, Shuai Bai, Shusheng Yang, Shijie Wang, Sinan Tan, Peng Wang, Junyang Lin, Chang Zhou, and Jingren Zhou. Qwen-vl: A frontier large vision-language model with versatile abilities. *arXiv preprint arXiv:2308.12966*, 2023. 3, 6, 7, 10
- [7] Tom Brown, Benjamin Mann, Nick Ryder, Melanie Subbiah, Jared D Kaplan, Prafulla Dhariwal, Arvind Neelakantan, Pranav Shyam, Girish Sastry, Amanda Askell, et al. Language models are few-shot learners. *NeurIPS*, 2020. 1
- [8] Soravit Changpinyo, Piyush Sharma, Nan Ding, and Radu

	Ground Truth	Generated w. MMFS	Generated w/o MMFS	Ground Truth	Generated w. MMFS	Generated w/o MMFS
[frame 0] text	Eddy is determined to hit the ball well. Eddy is holding the ball and talking to Pororo.	Eddy is determined to hit the ball well. Eddy is holding the ball and talking to Pororo.	Eddy is determined to hit the ball well. Eddy is holding the ball and talking to Pororo.	Wilma is talking to Betty, they are in a room together.	Wilma is talking to Betty, they are in a room together.	Wilma is talking to Betty, they are in a room together.
[frame 0] image						
[frame 1] text	Eddy seems very determined. Eddy threw the ball back. Eddy is getting ready to hit the ball.	Pororo smiles and ready to play.	Eddy tries to hit the ball but the ball cannot be go over the net.	Wilma and Betty are in a room, they are facing each other while Betty does all the talking to Wilma.	Wilma and Betty are standing in a room. Wilma is speaking to Betty. Betty looks at Wilma while touching her hand to her chin.	Wilma and Betty are standing in a room. Wilma speaks to Betty and Betty responds.
[frame 1] image						
[frame 2] text	Pororo is getting ready to catch the ball. Eddy is getting ready to hit the ball. Rody is holding the ball.	Pororo says he is going to play with the ball first. Pororo doesn't give the ball to Eddy.	Petty jumps and Loopy spins due to Cong's mistake.	Wilma and Betty are standing in a room. Betty is talking to Wilma. Wilma has her head turned toward Betty.	Wilma and Betty are standing in the room talking.	Betty and Wilma are having a conversation while standing in the living room.
[frame 2] image						
[frame 3] text	Rody is thinking about how to throw the ball. Rody is going to throw the ball.	Pororo is playing with the ball. Eddy is watching him playing. Pororo is throwing the ball at the wall and catching it again.	Eddy and Rody look disappointed. Cong picks up the ball.	Betty is standing in the room talking. Wilma is standing next to Betty.	Wilma and Betty are standing in a room speaking to each other.	Wilma and Betty are talking to each other in a room.
[frame 3] image						
[frame 4] text	Eddy is getting ready to throw the ball. Eddy is swinging the bat. Eddy looks very confident. Pororo is preparing to catch the ball.	Pororo is happy that Pororo got the ball. Eddy seems angry. Eddy also wants to play with the ball.	Eddy suggests Cong to give the ball to Eddy.	Wilma and Betty are standing in a room. Betty is holding her arms up while talking and Wilma turns to look at her.	Wilma is in the room. she is saying something she seems certain about.	Wilma and Betty are in the living room. Wilma is speaking to someone off screen. Betty looks at Wilma and then speaks to someone.
[frame 4] image						

Interleaved generating images and texts

Figure 9. Interleaved Image-Text Generation on PororoSV [49] and FlintstonesSV [28]. Each example consists of three columns. The first column is the ground-truth images and captions of all frames. The second column are the generated results with MMFS; And the last column are the results generated without MMFS. Only the caption and image of the first frame is given as condition during generation.

- Soricut. Conceptual 12m: Pushing web-scale image-text pre-training to recognize long-tail visual concepts. In *CVPR*, 2021. 6, 10
- [9] Jun Chen, Deyao Zhu, Xiaoqian Shen, Xiang Li, Zechun Liu, Pengchuan Zhang, Raghuraman Krishnamoorthi, Vikas Chandra, Yunyang Xiong, and Mohamed Elhoseiny. Minigpt-v2: large language model as a unified interface for vision-language multi-task learning. *arXiv preprint arXiv:2310.09478*, 2023. 7
- [10] Keqin Chen, Zhao Zhang, Weili Zeng, Richong Zhang, Feng Zhu, and Rui Zhao. Shikra: Unleashing multimodal llm’s referential dialogue magic. *arXiv preprint arXiv:2306.15195*, 2023. 3, 6, 7, 10
- [11] Xinlei Chen, Hao Fang, Tsung-Yi Lin, Ramakrishna Vedantam, Saurabh Gupta, Piotr Dollár, and C Lawrence Zitnick. Microsoft coco captions: Data collection and evaluation server. *arXiv preprint arXiv:1504.00325*, 2015. 6, 10, 11, 12
- [12] Zhe Chen, Yuchen Duan, Wenhai Wang, Junjun He, Tong Lu, Jifeng Dai, and Yu Qiao. Vision transformer adapter for dense predictions. In *ICLR*, 2022. 4
- [13] Christopher Clark and Matt Gardner. Simple and effective multi-paragraph reading comprehension. *arXiv preprint arXiv:1710.10723*, 2017. 10
- [14] Wenliang Dai, Junnan Li, Dongxu Li, AnthonyMeng Huat, Junqi Zhao, Weisheng Wang, Boyang Li, Pascale Fung, and Steven Hoi. Instructblip: Towards general-purpose vision-language models with instruction tuning. *arXiv preprint arXiv:2305.06500*, 2023. 6
- [15] Abhishek Das, Satwik Kottur, Khushi Gupta, Avi Singh, Deshraj Yadav, José MF Moura, Devi Parikh, and Dhruv Batra. Visual dialog. In *CVPR*, 2017. 6, 12
- [16] Ming Ding, Zhuoyi Yang, Wenyi Hong, Wendi Zheng, Chang Zhou, Da Yin, Junyang Lin, Xu Zou, Zhou Shao, Hongxia Yang, et al. Cogview: Mastering text-to-image generation via transformers. *NeurIPS*, 2021. 7
- [17] Ming Ding, Wendi Zheng, Wenyi Hong, and Jie Tang. Cogview2: Faster and better text-to-image generation via hierarchical transformers. *NeurIPS*, 2022. 7
- [18] Runpei Dong, Chunrui Han, Yuang Peng, Zekun Qi, Zheng Ge, Jinrong Yang, Liang Zhao, Jianjian Sun, Hongyu Zhou, Haoran Wei, et al. Dreamllm: Synergistic multimodal comprehension and creation. *arXiv preprint arXiv:2309.11499*, 2023. 1, 3, 6, 7, 10
- [19] Alexey Dosovitskiy, Lucas Beyer, Alexander Kolesnikov, Dirk Weissenborn, Xiaohua Zhai, Thomas Unterthiner, Mostafa Dehghani, Matthias Minderer, Georg Heigold, Sylvain Gelly, et al. An image is worth 16x16 words: Transformers for image recognition at scale. In *ICLR*, 2020. 3
- [20] Patrick Esser, Robin Rombach, and Bjorn Ommer. Taming transformers for high-resolution image synthesis. In *CVPR*, 2021. 8
- [21] Yuxin Fang, Wen Wang, Binhui Xie, Quan Sun, Ledell Wu, Xinggang Wang, Tiejun Huang, Xinlong Wang, and Yue Cao. Eva: Exploring the limits of masked visual representation learning at scale. *arXiv preprint arXiv:2211.07636*, 2022. 1
- [22] Yuxin Fang, Quan Sun, Xinggang Wang, Tiejun Huang, Xinlong Wang, and Yue Cao. Eva-02: A visual representation for neon genesis. *arXiv preprint arXiv:2303.11331*, 2023. 1
- [23] Zhangyin Feng, Yuchen Ren, Xinmiao Yu, Xiaocheng Feng, Duyu Tang, Shuming Shi, and Bing Qin. Improved visual story generation with adaptive context modeling. *arXiv preprint arXiv:2305.16811*, 2023. 8
- [24] Samir Yitzhak Gadre, Gabriel Ilharco, Alex Fang, Jonathan Hayase, Georgios Smyrnis, Thao Nguyen, Ryan Marten, Mitchell Wortsman, Dhruva Ghosh, Jieyu Zhang, et al. Datacomp: In search of the next generation of multimodal datasets. *arXiv preprint arXiv:2304.14108*, 2023. 2
- [25] Oran Gafni, Adam Polyak, Oron Ashual, Shelly Sheynin, Devi Parikh, and Yaniv Taigman. Make-a-scene: Scene-based text-to-image generation with human priors. In *ECCV*, 2022. 7
- [26] Xinyang Geng and Hao Liu. Openllama: An open reproduction of llama, 2023. 8
- [27] Yash Goyal, Tejas Khot, Douglas Summers-Stay, Dhruv Batra, and Devi Parikh. Making the v in vqa matter: Elevating the role of image understanding in visual question answering. In *CVPR*, 2017. 6, 10, 12
- [28] Tanmay Gupta, Dustin Schwenk, Ali Farhadi, Derek Hoiem, and Aniruddha Kembhavi. Imagine this! scripts to compositions to videos. In *ECCV*, 2018. 8, 12, 15, 16
- [29] Danna Gurari, Qing Li, Abigale J Stangl, Anhong Guo, Chi Lin, Kristen Grauman, Jiebo Luo, and Jeffrey P Bigham. Vizwiz grand challenge: Answering visual questions from blind people. In *CVPR*, 2018. 6, 12
- [30] Yaru Hao, Haoyu Song, Li Dong, Shaohan Huang, Zewen Chi, Wenhui Wang, Shuming Ma, and Furu Wei. Language models are general-purpose interfaces. *arXiv preprint arXiv:2206.06336*, 2022. 6
- [31] Martin Heusel, Hubert Ramsauer, Thomas Unterthiner, Bernhard Nessler, and Sepp Hochreiter. Gans trained by a two time-scale update rule converge to a local nash equilibrium. *NeurIPS*, 2017. 7, 11, 12
- [32] Jonathan Ho and Tim Salimans. Classifier-free diffusion guidance. *arXiv preprint arXiv:2207.12598*, 2022. 10, 11
- [33] Shaohan Huang, Li Dong, Wenhui Wang, Yaru Hao, Saksham Singhal, Shuming Ma, Tengchao Lv, Lei Cui, Owais Khan Mohammed, Qiang Liu, et al. Language is not all you need: Aligning perception with language models. *arXiv preprint arXiv:2302.14045*, 2023. 2, 6
- [34] Ting-Hao K. Huang, Francis Ferraro, Nasrin Mostafazadeh, Ishan Misra, Jacob Devlin, Aishwarya Agrawal, Ross Girshick, Xiaodong He, Pushmeet Kohli, Dhruv Batra, et al. Visual storytelling. In *NAACL*, 2016. 7, 8, 11, 12
- [35] Drew A Hudson and Christopher D Manning. Gqa: A new dataset for real-world visual reasoning and compositional question answering. In *CVPR*, 2019. 6, 12
- [36] IDEFICS. Introducing idefics: An open reproduction of state-of-the-art visual language model. <https://huggingface.co/blog/idefics>, 2023. 6
- [37] Gabriel Ilharco, Mitchell Wortsman, Ross Wightman, Cade Gordon, Nicholas Carlini, Rohan Taori, Achal Dave,

- Vaishaal Shankar, Hongseok Namkoong, John Miller, Hananeh Hajishirzi, Ali Farhadi, and Ludwig Schmidt. Openclip, 2021. [1](#), [2](#)
- [38] Jitesh Jain, Jiachen Li, Mang Tik Chiu, Ali Hassani, Nikita Orlov, and Humphrey Shi. Oneformer: One transformer to rule universal image segmentation. In *CVPR*, 2023. [7](#), [8](#)
- [39] Chao Jia, Yinfei Yang, Ye Xia, Yi-Ting Chen, Zarana Parekh, Hieu Pham, Quoc Le, Yun-Hsuan Sung, Zhen Li, and Tom Duerig. Scaling up visual and vision-language representation learning with noisy text supervision. In *ICML*, 2021. [2](#)
- [40] Yang Jin, Kun Xu, Kun Xu, Liwei Chen, Chao Liao, Jianchao Tan, Quzhe Huang, Bin Chen, Chenyi Lei, An Liu, Chengru Song, Xiaoqiang Lei, Di Zhang, Wenwu Ou, Kun Gai, and Yadong Mu. Unified language-vision pretraining in llm with dynamic discrete visual tokenization. *arXiv preprint arXiv:2309.04669*, 2023. [1](#)
- [41] Kushal Kafle, Brian Price, Scott Cohen, and Christopher Kanan. Dvqa: Understanding data visualizations via question answering. In *Proceedings of the IEEE conference on computer vision and pattern recognition*, pages 5648–5656, 2018. [10](#)
- [42] Sahar Kazemzadeh, Vicente Ordonez, Mark Matten, and Tamara Berg. Referitgame: Referring to objects in photographs of natural scenes. In *EMNLP*, 2014. [7](#), [10](#), [12](#)
- [43] Jing Yu Koh, Daniel Fried, and Ruslan Salakhutdinov. Generating images with multimodal language models. *arXiv preprint arXiv:2305.17216*, 2023. [1](#), [3](#), [7](#), [8](#), [11](#)
- [44] Jonathan Krause, Justin Johnson, Ranjay Krishna, and Li Fei-Fei. A hierarchical approach for generating descriptive image paragraphs. In *CVPR*, 2017. [6](#), [11](#), [12](#)
- [45] Hugo Laurençon, Lucile Saulnier, Léo Tronchon, Stas Bekman, Amanpreet Singh, Anton Lozhkov, Thomas Wang, Siddharth Karamcheti, Alexander M Rush, Douwe Kiela, et al. Obelics: An open web-scale filtered dataset of interleaved image-text documents. In *Thirty-seventh Conference on Neural Information Processing Systems Datasets and Benchmarks Track*, 2023. [2](#), [7](#)
- [46] Junnan Li, Ramprasaath Selvaraju, Akhilesh Gotmare, Shafiq Joty, Caiming Xiong, and Steven Chu Hong Hoi. Align before fuse: Vision and language representation learning with momentum distillation. *NeurIPS*, 2021. [2](#)
- [47] Junnan Li, Dongxu Li, Caiming Xiong, and Steven Hoi. Blip: Bootstrapping language-image pre-training for unified vision-language understanding and generation. In *ICML*, 2022. [10](#), [11](#)
- [48] Junnan Li, Dongxu Li, Silvio Savarese, and Steven Hoi. Blip-2: Bootstrapping language-image pre-training with frozen image encoders and large language models. *arXiv preprint arXiv:2301.12597*, 2023. [1](#), [2](#), [3](#), [4](#), [6](#), [10](#)
- [49] Yitong Li, Zhe Gan, Yelong Shen, Jingjing Liu, Yu Cheng, Yuexin Wu, Lawrence Carin, David Carlson, and Jianfeng Gao. Storygan: A sequential conditional gan for story visualization. In *CVPR*, 2019. [8](#), [11](#), [12](#), [15](#), [16](#)
- [50] Yanghao Li, Haoqi Fan, Ronghang Hu, Christoph Feichtenhofer, and Kaiming He. Scaling language-image pre-training via masking. In *CVPR*, 2023. [2](#)
- [51] Tsung-Yi Lin, Michael Maire, Serge Belongie, James Hays, Pietro Perona, Deva Ramanan, Piotr Dollár, and C Lawrence Zitnick. Microsoft coco: Common objects in context. In *ECCV*, 2014. [7](#), [12](#)
- [52] Haotian Liu, Chunyuan Li, Yuheng Li, and Yong Jae Lee. Improved baselines with visual instruction tuning. *arXiv preprint arXiv:2310.03744*, 2023. [6](#), [7](#), [10](#)
- [53] Haotian Liu, Chunyuan Li, Qingyang Wu, and Yong Jae Lee. Visual instruction tuning. *arXiv preprint arXiv:2304.08485*, 2023. [1](#), [2](#), [3](#), [4](#)
- [54] Calvin Luo. Understanding diffusion models: A unified perspective. *arXiv preprint arXiv:2208.11970*, 2022. [4](#)
- [55] Tengchao Lv, Yupan Huang, Jingye Chen, Lei Cui, Shuming Ma, Yaoyao Chang, Shaohan Huang, Wenhui Wang, Li Dong, Weiyao Luo, et al. Kosmos-2.5: A multimodal literate model. *arXiv preprint arXiv:2309.11419*, 2023. [2](#), [3](#)
- [56] Adyasha Maharana and Mohit Bansal. Integrating visuospatial, linguistic and commonsense structure into story visualization. *arXiv preprint arXiv:2110.10834*, 2021. [11](#)
- [57] Adyasha Maharana, Darryl Hannan, and Mohit Bansal. Storydall-e: Adapting pretrained text-to-image transformers for story continuation. In *ECCV*, 2022. [8](#)
- [58] Junhua Mao, Jonathan Huang, Alexander Toshev, Oana Camburu, Alan L Yuille, and Kevin Murphy. Generation and comprehension of unambiguous object descriptions. In *CVPR*, 2016. [7](#), [10](#), [12](#), [13](#)
- [59] Kenneth Marino, Mohammad Rastegari, Ali Farhadi, and Roozbeh Mottaghi. Ok-vqa: A visual question answering benchmark requiring external knowledge. In *CVPR*, 2019. [6](#), [8](#), [12](#)
- [60] Ahmed Masry, Do Xuan Long, Jia Qing Tan, Shafiq Joty, and Enamul Hoque. Chartqa: A benchmark for question answering about charts with visual and logical reasoning. *arXiv preprint arXiv:2203.10244*, 2022. [10](#)
- [61] Minesh Mathew, Viraj Bagal, Rubèn Tito, Dimosthenis Karatzas, Ernest Valveny, and CV Jawahar. Infographicvqa. In *Proceedings of the IEEE/CVF Winter Conference on Applications of Computer Vision*, pages 1697–1706, 2022. [10](#)
- [62] Anand Mishra, Shashank Shekhar, Ajeet Kumar Singh, and Anirban Chakraborty. Ocr-vqa: Visual question answering by reading text in images. In *ICDAR*, pages 947–952. IEEE, 2019. [10](#)
- [63] Alex Nichol, Prafulla Dhariwal, Aditya Ramesh, Pranav Shyam, Pamela Mishkin, Bob McGrew, Ilya Sutskever, and Mark Chen. Glide: Towards photorealistic image generation and editing with text-guided diffusion models. *arXiv preprint arXiv:2112.10741*, 2021. [7](#)
- [64] OpenAI. Gpt-4 technical report. *arXiv preprint arXiv:2303.08774*, 2023. [1](#), [2](#)
- [65] TB OpenAI. Chatgpt: Optimizing language models for dialogue. *OpenAI*, 2022. [2](#)
- [66] Xichen Pan, Pengda Qin, Yuhong Li, Hui Xue, and Wenhui Chen. Synthesizing coherent story with auto-regressive latent diffusion models. *arXiv preprint arXiv:2211.10950*, 2022. [8](#), [11](#)
- [67] Zhiliang Peng, Wenhui Wang, Li Dong, Yaru Hao, Shaohan Huang, Shuming Ma, and Furu Wei. Kosmos-2: Ground-

- ing multimodal large language models to the world. *arXiv preprint arXiv:2306.14824*, 2023. 6
- [68] Bryan A Plummer, Liwei Wang, Chris M Cervantes, Juan C Caicedo, Julia Hockenmaier, and Svetlana Lazebnik. Flickr30k entities: Collecting region-to-phrase correspondences for richer image-to-sentence models. In *ICCV*, 2015. 6, 11, 12
- [69] Jordi Pont-Tuset, Jasper Uijlings, Soravit Changpinyo, Radu Soricut, and Vittorio Ferrari. Connecting vision and language with localized narratives. In *ECCV*, 2020. 7, 12
- [70] Alec Radford, Jong Wook Kim, Chris Hallacy, Aditya Ramesh, Gabriel Goh, Sandhini Agarwal, Girish Sastry, Amanda Askell, Pamela Mishkin, Jack Clark, et al. Learning transferable visual models from natural language supervision. In *ICML*, 2021. 1, 2, 4, 5, 7, 8, 11, 12
- [71] Aditya Ramesh, Mikhail Pavlov, Gabriel Goh, Scott Gray, Chelsea Voss, Alec Radford, Mark Chen, and Ilya Sutskever. Zero-shot text-to-image generation. In *ICML*, 2021. 1, 2, 7
- [72] Aditya Ramesh, Prafulla Dhariwal, Alex Nichol, Casey Chu, and Mark Chen. Hierarchical text-conditional image generation with clip latents. *arXiv preprint arXiv:2204.06125*, 2022. 7
- [73] Robin Rombach, Andreas Blattmann, Dominik Lorenz, Patrick Esser, and Björn Ommer. High-resolution image synthesis with latent diffusion models. In *CVPR*, 2022. 8
- [74] Robin Rombach, Andreas Blattmann, Dominik Lorenz, Patrick Esser, and Björn Ommer. High-resolution image synthesis with latent diffusion models. In *CVPR*, 2022. 1, 2, 4, 5, 7
- [75] Chitwan Saharia, William Chan, Saurabh Saxena, Lala Li, Jay Whang, Emily L Denton, Kamyar Ghasemipour, Raphael Gontijo Lopes, Burcu Karagol Ayan, Tim Salimans, et al. Photorealistic text-to-image diffusion models with deep language understanding. *NeurIPS*, 2022. 7
- [76] Christoph Schuhmann, Romain Beaumont, Richard Vencu, Cade Gordon, Ross Wightman, Mehdi Cherti, Theo Coombes, Aarush Katta, Clayton Mullis, Mitchell Wortsman, et al. Laion-5b: An open large-scale dataset for training next generation image-text models. *NeurIPS*, 2022. 2, 6, 8, 10
- [77] Christoph Schuhmann, Andreas Köpf, Richard Vencu, Theo Coombes, and Romain Beaumont. Laion coco: 600m synthetic captions from laion2b-en. <https://laion.ai/blog/laion-coco/>, 2022. 6, 8, 10
- [78] Shuai Shao, Zeming Li, Tianyuan Zhang, Chao Peng, Gang Yu, Xiangyu Zhang, Jing Li, and Jian Sun. Objects365: A large-scale, high-quality dataset for object detection. In *ICCV*, 2019. 6, 10
- [79] Oleksii Sidorov, Ronghang Hu, Marcus Rohrbach, and Amanpreet Singh. Textcaps: a dataset for image captioning with reading comprehension. In *ECCV*, pages 742–758. Springer, 2020. 10
- [80] Amanpreet Singh, Vivek Natarajan, Meet Shah, Yu Jiang, Xinlei Chen, Dhruv Batra, Devi Parikh, and Marcus Rohrbach. Towards vqa models that can read. In *CVPR*, 2019. 6, 12, 13
- [81] Quan Sun, Yufeng Cui, Xiaosong Zhang, Fan Zhang, Qiyang Yu, Zhengxiong Luo, Yueze Wang, Yongming Rao, Jingjing Liu, Tiejun Huang, et al. Generative multimodal models are in-context learners. *arXiv preprint arXiv:2312.13286*, 2023. 6
- [82] Quan Sun, Yuxin Fang, Ledell Wu, Xinlong Wang, and Yue Cao. Eva-clip: Improved training techniques for clip at scale. *arXiv preprint arXiv:2303.15389*, 2023. 1, 2
- [83] Quan Sun, Qiyang Yu, Yufeng Cui, Fan Zhang, Xiaosong Zhang, Yueze Wang, Hongcheng Gao, Jingjing Liu, Tiejun Huang, and Xinlong Wang. Generative pretraining in multimodality. *arXiv preprint arXiv:2307.05222*, 2023. 1, 3, 6, 7, 9, 10
- [84] Han Tian, Chaoliang Zeng, Zhenghang Ren, Di Chai, Junxue Zhang, Kai Chen, and Qiang Yang. Sphinx: Enabling privacy-preserving online learning over the cloud. In *2022 IEEE Symposium on Security and Privacy (SP)*, 2022. 2, 3
- [85] Hugo Touvron, Thibaut Lavril, Gautier Izacard, Xavier Martinet, Marie-Anne Lachaux, Timothée Lacroix, Baptiste Rozière, Naman Goyal, Eric Hambro, Faisal Azhar, et al. Llama: Open and efficient foundation language models. *arXiv preprint arXiv:2302.13971*, 2023. 4
- [86] Aaron Van Den Oord, Oriol Vinyals, et al. Neural discrete representation learning. *NeurIPS*, 2017. 3
- [87] Ramakrishna Vedantam, C. Lawrence Zitnick, and Devi Parikh. Cider: Consensus-based image description evaluation. In *CVPR*, 2015. 12
- [88] Peng Wang, An Yang, Rui Men, Junyang Lin, Shuai Bai, Zhikang Li, Jianxin Ma, Chang Zhou, Jingren Zhou, and Hongxia Yang. Ofa: Unifying architectures, tasks, and modalities through a simple sequence-to-sequence learning framework. In *ICML*, 2022. 7
- [89] Tengfei Wang, Ting Zhang, Bo Zhang, Hao Ouyang, Dong Chen, Qifeng Chen, and Fang Wen. Pretraining is all you need for image-to-image translation. *arXiv preprint arXiv:2205.12952*, 2022. 8
- [90] Wenhai Wang, Zhe Chen, Xiaokang Chen, Jiannan Wu, Xizhou Zhu, Gang Zeng, Ping Luo, Tong Lu, Jie Zhou, Yu Qiao, et al. Visionllm: Large language model is also an open-ended decoder for vision-centric tasks. *arXiv preprint arXiv:2305.11175*, 2023. 2, 4, 7
- [91] Weiyun Wang, Min Shi, Qingyun Li, Wenhai Wang, Zhenghang Huang, Linjie Xing, Zhe Chen, Hao Li, Xizhou Zhu, Zhiguo Cao, et al. The all-seeing project: Towards panoptic visual recognition and understanding of the open world. *arXiv preprint arXiv:2308.01907*, 2023. 2, 4
- [92] Xinyu Wang, Yuliang Liu, Chunhua Shen, Chun Chet Ng, Canjie Luo, Lianwen Jin, Chee Seng Chan, Anton van den Hengel, and Liangwei Wang. On the general value of evidence, and bilingual scene-text visual question answering. In *CVPR*, pages 10126–10135, 2020. 10
- [93] Zirui Wang, Jiahui Yu, Adams Wei Yu, Zihang Dai, Yulia Tsvetkov, and Yuan Cao. Simvlm: Simple visual language model pretraining with weak supervision. *arXiv preprint arXiv:2108.10904*, 2021. 2
- [94] Yinfei Yang, Daniel Cer, Amin Ahmad, Mandy Guo, Jax Law, Noah Constant, Gustavo Hernandez Abrego, Steve

- Yuan, Chris Tar, Yun-Hsuan Sung, et al. Multilingual universal sentence encoder for semantic retrieval. In *Proceedings of the 58th Annual Meeting of the Association for Computational Linguistics: System Demonstrations*, 2020. 7
- [95] Jiabo Ye, Anwen Hu, Haiyang Xu, Qinghao Ye, Ming Yan, Yuhao Dan, Chenlin Zhao, Guohai Xu, Chenliang Li, Junfeng Tian, Qian Qi, Ji Zhang, and Fei Huang. mplug-docowl: Modularized multimodal large language model for document understanding, 2023. 6
- [96] Haoxuan You, Haotian Zhang, Zhe Gan, Xianzhi Du, Bowen Zhang, Zirui Wang, Liangliang Cao, Shih-Fu Chang, and Yinfei Yang. Ferret: Refer and ground anything anywhere at any granularity. *arXiv preprint arXiv:2310.07704*, 2023. 7
- [97] Jiahui Yu, Zirui Wang, Vijay Vasudevan, Legg Yeung, Mojtaba Seyedhosseini, and Yonghui Wu. Coca: Contrastive captioners are image-text foundation models. *arXiv preprint arXiv:2205.01917*, 2022. 2
- [98] Jiahui Yu, Yuanzhong Xu, Jing Yu Koh, Thang Luong, Gunjan Baid, Zirui Wang, Vijay Vasudevan, Alexander Ku, Yinfei Yang, Burcu Karagol Ayan, et al. Scaling autoregressive models for content-rich text-to-image generation. *arXiv preprint arXiv:2206.10789*, 2022. 7
- [99] Lili Yu, Bowen Shi, Ramakanth Pasunuru, Benjamin Muller, Olga Golovneva, Tianlu Wang, Arun Babu, Binh Tang, Brian Karrer, Shelly Sheynin, et al. Scaling autoregressive multi-modal models: Pretraining and instruction tuning. *arXiv preprint arXiv:2309.02591*, 2023. 2, 3, 6, 7
- [100] Lvmin Zhang, Anyi Rao, and Maneesh Agrawala. Adding conditional control to text-to-image diffusion models. In *ICCV*, 2023. 7, 8, 11
- [101] Pan Zhang, Xiaoyi Dong Bin Wang, Yuhang Cao, Chao Xu, Linke Ouyang, Zhiyuan Zhao, Shuangrui Ding, Songyang Zhang, Haodong Duan, Hang Yan, et al. Internlm-xcomposer: A vision-language large model for advanced text-image comprehension and composition. *arXiv preprint arXiv:2309.15112*, 2023. 3
- [102] Yanzhe Zhang, Ruiyi Zhang, Jiuxiang Gu, Yufan Zhou, Nedim Lipka, Diyi Yang, and Tong Sun. Llavir: Enhanced visual instruction tuning for text-rich image understanding. *arXiv preprint arXiv:2306.17107*, 2023. 10
- [103] Haozhe Zhao, Zefan Cai, Shuzheng Si, Xiaojian Ma, Kaikai An, Liang Chen, Zixuan Liu, Sheng Wang, Wenjuan Han, and Baobao Chang. Mmicl: Empowering vision-language model with multi-modal in-context learning. *arXiv preprint arXiv:2309.07915*, 2023. 3
- [104] Kaizhi Zheng, Xuehai He, and Xin Eric Wang. Minigpt-5: Interleaved vision-and-language generation via generative vokens. *arXiv preprint arXiv:2310.02239*, 2023. 8, 11
- [105] Lianmin Zheng, Wei-Lin Chiang, Ying Sheng, Siyuan Zhuang, Zhanghao Wu, Yonghao Zhuang, Zi Lin, Zhuohan Li, Dacheng Li, Eric. P Xing, Hao Zhang, Joseph E. Gonzalez, and Ion Stoica. Judging llm-as-a-judge with mt-bench and chatbot arena, 2023. 4, 5
- [106] Bolei Zhou, Hang Zhao, Xavier Puig, Sanja Fidler, Adela Barriuso, and Antonio Torralba. Scene parsing through ade20k dataset. In *CVPR*, 2017. 8, 12, 14
- [107] Deyao Zhu, Jun Chen, Xiaoqian Shen, Xiang Li, and Mohamed Elhoseiny. Minigpt-4: Enhancing vision-language understanding with advanced large language models. *arXiv preprint arXiv:2304.10592*, 2023. 3
- [108] Jinguo Zhu, Xiaohan Ding, Yixiao Ge, Yuying Ge, Sijie Zhao, Hengshuang Zhao, Xiaohua Wang, and Ying Shan. Vl-gpt: A generative pre-trained transformer for vision and language understanding and generation. *arXiv preprint arXiv:2312.09251*, 2023. 6, 7
- [109] Wanrong Zhu, Jack Hessel, Anas Awadalla, Samir Yitzhak Gadre, Jesse Dodge, Alex Fang, Youngjae Yu, Ludwig Schmidt, William Yang Wang, and Yejin Choi. Multimodal c4: An open, billion-scale corpus of images interleaved with text. *arXiv preprint arXiv:2304.06939*, 2023. 2, 6, 8, 10
- [110] Xizhou Zhu, Weijie Su, Lewei Lu, Bin Li, Xiaogang Wang, and Jifeng Dai. Deformable detr: Deformable transformers for end-to-end object detection. In *ICLR*, 2020. 2, 4
- [111] Xizhou Zhu, Jinguo Zhu, Hao Li, Xiaoshi Wu, Xiaogang Wang, Hongsheng Li, Xiaohua Wang, and Jifeng Dai. Uni-perceiver: Pre-training unified architecture for generic perception for zero-shot and few-shot tasks. *arXiv preprint arXiv:2112.01522*, 2021. 2